ACS central science

Research Article

Cite This: ACS Cent. Sci. 2019, 5, 808−820

http://pubs.acs.org/journal/acscii

A Specific, Glycomimetic Langerin Ligand for Human Langerhans Cell Targeting

Eike-Christian Wamhoff,[†,‡] Jessica Schulze,[†,‡,#] Lydia Bellmann,[§,#] Mareike Rentzsch,[†] Gunnar Bachem,[∥] Felix F. Fuchsberger,[†,○] Juliane Rademacher,[†] Martin Hermann,[⊥] Barbara Del Frari,[▽] Rob van Dalen,[○] David Hartmann,[†] Nina M. van Sorge,[○] Oliver Seitz,[∥] Patrizia Stoitzner,[§] and Christoph Rademacher*[,†,‡]

[†]Department of Biomolecular Systems, Max Planck Institute of Colloids and Interfaces, 14424 Potsdam, Germany

[‡]Department of Biology, Chemistry and Pharmacy, Freie Universität Berlin, 14195 Berlin, Germany

[§]Department of Dermatology, Venereology and Allergology, [⊥]Department of Anesthesiology and Intensive Care Medicine, and [▽]Department of Plastic, Reconstructive and Aesthetic Surgery, Medical University of Innsbruck, 6020 Innsbruck, Austria

[∥]Department of Chemistry, Humboldt-Universität zu Berlin, 12489 Berlin, Germany

[○]Medical Microbiology, University Medical Center Utrecht, Utrecht University, 3584 CX Utrecht, Netherlands

Supporting Information

ABSTRACT: Langerhans cells are a subset of dendritic cells residing in the epidermis of the human skin. As such, they are key mediators of immune regulation and have emerged as prime targets for novel transcutaneous cancer vaccines. Importantly, the induction of protective T cell immunity by these vaccines requires the efficient and specific delivery of both tumor-associated antigens and adjuvants. Langerhans cells uniquely express Langerin (CD207), an endocytic C-type lectin receptor. Here, we report the discovery of a specific, glycomimetic Langerin ligand employing a heparin-inspired design strategy and structural characterization by NMR spectroscopy and molecular docking. The conjugation of this glycomimetic to liposomes enabled the specific and efficient targeting of Langerhans cells in the human skin. We further demonstrate the doxorubicin-mediated killing of a Langerin$^+$ monocyte cell line, highlighting its therapeutic and diagnostic potential in Langerhans cell histiocytosis, caused by the abnormal proliferation of Langerin$^+$ myeloid progenitor cells. Overall, our delivery platform provides superior versatility over antibody-based approaches and novel modalities to overcome current limitations of dendritic cell-targeted immuno- and chemotherapy.

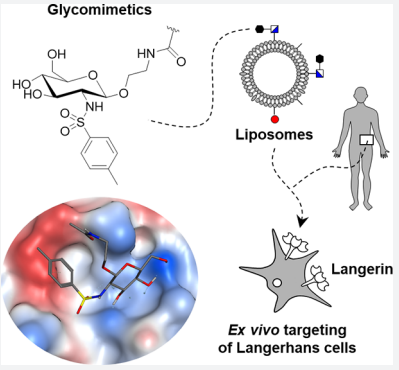

INTRODUCTION

The human skin is an attractive vaccination site due to the high density of immune cells compared to other organs such as the muscle.[1] The highly efficacious and cost-effective small pox vaccine was first used via this administration route and has proven its feasibility.[2] The skin contains several subsets of dendritic cells (DCs), immune cells that are specialized in the internalization of pathogens and the presentation of antigens to induce T cell responses.[3] Langerhans cells (LCs) constitute a subset of DCs residing in the epidermis of the stratified as well as the mucosal skin. Following their activation, LCs migrate to the draining lymph nodes to elicit systemic immune responses.[4] Because of their localization in the epidermis and their ability to cross-present exogenous antigens to cytotoxic T cells, LCs have emerged as promising targets for transcutaneous vaccination strategies.[5−7] Various approaches such as microneedles or thermal ablation have been explored to overcome the stratum corneum and thereby facilitate antigen delivery to the skin.[1]

Sipuleucel-T, an adoptive cell therapy for prostate cancer, has provided proof of concept for the induction of protective cytotoxic T cell responses against tumor-associated antigens (TAAs) by myeloid immune cells.[8] Moreover, the adoptive transfer of monocyte-derived DCs into melanoma patients has been demonstrated to elicit TAA-specific T cell immunity.[9] As ex vivo strategies remain laborious and expensive, the focus has shifted toward the delivery of antigens in situ.[10] Intriguingly, DCs express several endocytic receptors including chemokine receptors, scavenger receptors, and C-type lectin receptors (CLRs) that promote the internalization and cross-presentation of antigens.[11−13] Pioneered by Steinman et al., the use of antibody−antigen conjugates targeting CLRs such as DEC-205, DC-SIGN, and DNGR-1 represents an established strategy to deliver antigens to DCs and has been translated into clinical trials.[14−17] These investigations helped identify several parameters that shape cytotoxic T cell immunity and

Received: January 29, 2019
Published: May 10, 2019

DOI: 10.1021/acscentsci.9b00093
ACS Cent. Sci. 2019, 5, 808−820

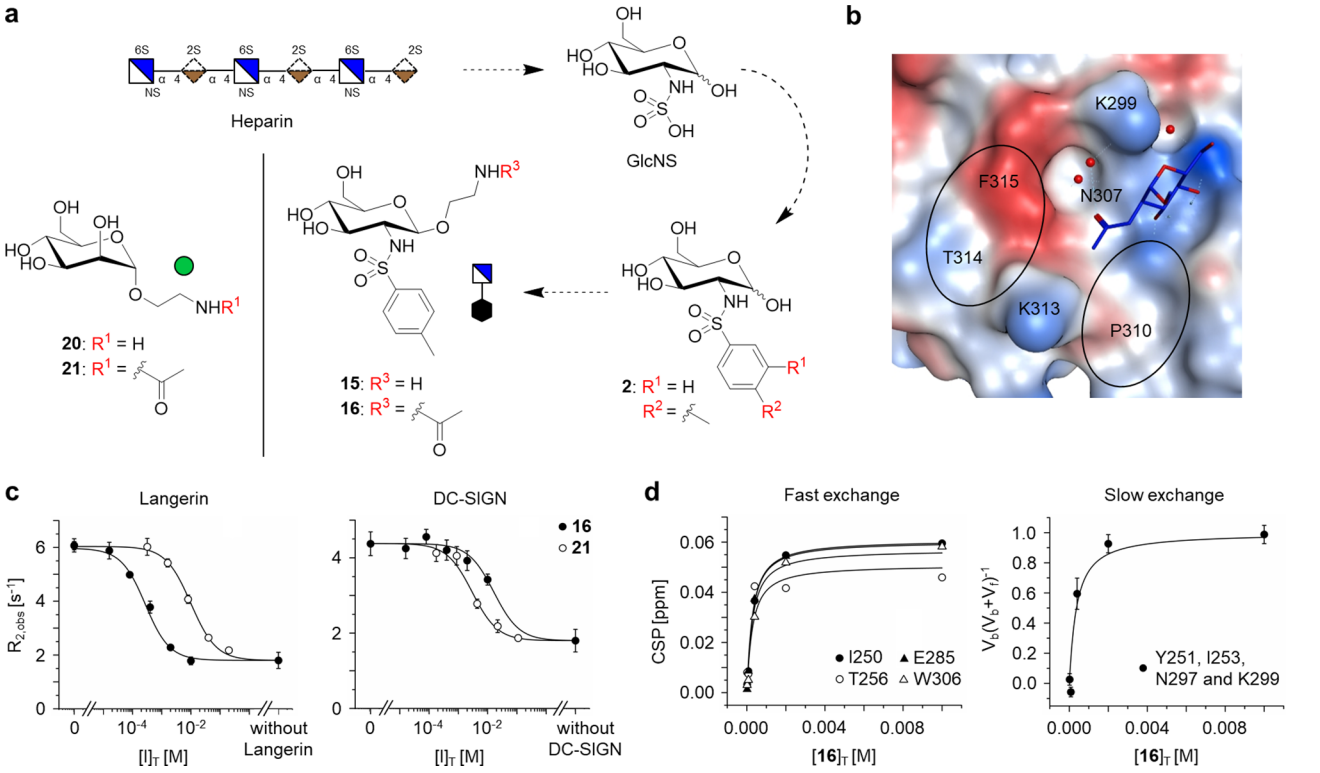

Figure 1. Heparin-inspired design of glycomimetic targeting ligands for Langerin. (a) The heparin-derived monosaccharide GlcNS was identified as a favorable scaffold for glycomimetic ligand design. The design of GlcNS analogues lead to the discovery of glycomimetic targeting ligand **15**. **15** bears an ethylamino linker in β-orientation of C1 for conjugation to the delivery platform. **20** served as a Man-based reference molecule throughout this study. (b) On the basis of the binding mode of GlcNAc (PDB code: 4N32), potentially favorable cation-π or $\pi-\pi$ interactions between small substituents and the Langerin binding site were explored.[40] The receptor surface is colored according to its lipophilicity (lipophilic: red, hydrophilic: blue). (c) ^{19}F R_2-filtered NMR experiments revealed a 42-fold affinity increase for model ligand **16** (K_I = 0.24 ± 0.03 mM) over Man-based reference molecule **21** (K_I = 10 ± 1 mM). Additionally, **16** displayed an encouraging specificity against DC-SIGN ($K_{I,DC\text{-}SIGN}$ = 15 ± 3 mM). (d) The affinity of **16** for Langerin was validated in ^{15}N HSQC NMR experiments analyzing resonances in the fast ($K_{D,fast}$ = 0.23 ± 0.07 mM) and the slow ($K_{D,slow}$ = 0.3 ± 0.1 mM) exchange regime.

guide the development of next-generation cancer vaccines. First, the activation of DCs by coadministration of adjuvants such as Toll-like receptor (TLR) or RIG-I-like receptor agonists is required to avoid tolerance induction.[18] Furthermore, the choice of delivery platform and targeting ligand influence the efficiency of antigen internalization, processing, and cross-presentation by DCs.[19−22]

Finally, the specific targeting of individual DC subsets is essential as off-target delivery of antigens and adjuvants may result in adverse effects or compromised cytotoxic T cell immunity.[23,24] Consequently, DC subset-specific receptors such as the CLRs Langerin and DNGR-1 as well as the chemokine receptor XCR1 have become a focal point for the development of novel immunotherapies.[13,17] In healthy humans, Langerin (CD207) is exclusively expressed on LCs and has been shown to promote the endocytosis and cross-presentation of antigens to prime cytotoxic T cells.[4,22] The CLR thus represents an attractive target receptor for transcutaneous vaccination strategies.[25]

Furthermore, Langerin-mediated targeting is potentially relevant in Langerhans cell histiocytosis (LCH). LCH, one of the most common pediatric cancers, is caused by the abnormal proliferation of Langerin$^+$ myeloid progenitor cells and manifests as lesions of the skin, bone marrow, and lungs as wells as other organs.[26] Clinical manifestation are highly variable, and despite advances in elucidating the mechanism of disease progression and chemotherapy, survival rates remain below 50%.[27] As lesions consist of up to 70% LCH cells of varying phenotype, targeted delivery holds both therapeutic and diagnostic potential by reducing adverse effects and facilitating the characterization of the disease in individual patients.[28]

In this study, we pursued the development of targeted nanoparticles as an antigen or chemotherapeutics delivery platform for LCs as an alternative to antibody-based approaches. Liposomes represent versatile nanoparticles that have been approved for the delivery of chemotherapeutics in Kaposi's sarcoma and allow for the coformulation of adjuvants.[29,30] They can be targeted to glycan-binding proteins (GBPs) including CLRs or sialic acid-binding immunoglobulin-like lectins (Siglecs) expressed on immune cells using glycans or glycomimetic ligands.[31−33]

Glycan recognition by Langerin is Ca^{2+}- as well as pH-dependent and consequently abrogated in the early endosome, thereby influencing lysosomal antigen degradation.[34] This release mechanism simultaneously increases the internalization capacity of LCs as unbound Langerin has been shown to recycle to the plasma membrane.[35] Hence, the use of glycans or glycomimetics provides advantages over antibody-based approaches which potentially suffer from inefficient ligand release.[20,21] As glycans are typically recognized by several CLRs or other GBPs, they do not provide the specificity required to target individual DC subsets.[36] Additionally, glycan−Langerin interactions display low affinities insufficient

DOI: 10.1021/acscentsci.9b00093
ACS Cent. Sci. 2019, 5, 808−820

Table 1. Structure−Activity Relationship and Specificity against DC-SIGN

	Langerin			DC-SIGN	
structure	K_I [mM]	K_D [mM]	relative potency[a]	K_I [mM]	specificity
2	0.32 ± 0.05	0.46 ± 0.04 0.5 ± 0.2[b]	31	17 ± 1	53
16	0.24 ± 0.03	0.23 ± 0.07 0.3 ± 0.1[b]	42	15 ± 3	63
Man	4.5 ± 0.5[c]	6.5 ± 0.2[c]	2.2	3.0 ± 0.3	0.67
21	10 ± 1	12 ± 1	1.0	2.7 ± 0.3	0.27

[a]The relative potency was calculated utilizing the K_I value determined for **21**. [b]The value was determined from integrals V of resonances observed to be in slow exchange. [c]The value was previously published.[54]

to promote the endocytosis of liposomes.[37−40] This renders the design of potent and specific glycomimetic ligands essential for the development of an antigen delivery platform for LCs. The carbohydrate binding sites of CLRs are hydrophilic and solvent-exposed which has impeded the discovery of drug-like molecule ligands.[41,42] While mono- and oligosaccharides represent attractive scaffolds, the synthesis of carbohydrates and structural glycomimetics is generally considered onerous.[43,44] Nevertheless, individual reports have demonstrated the feasibility of ligand design for these challenging target receptors and other GBPs.[45−49] Many of these reports highlight the utility of concepts from rational and fragment-based drug discovery for glycomimetic ligand design.

Here, we present the discovery of the first micromolar glycomimetic ligand for Langerin. We rationally designed heparin-derived monosaccharide analogues and analyzed their binding via NMR spectroscopy and molecular docking. The targeting ligand facilitated the endocytosis of liposomes by LCs and provided remarkable specificity over other GBPs in a physiologically relevant ex vivo skin model. Our findings demonstrate for the first time the CLR-mediated targeting of nanoparticles to individual immune cell subsets using glycomimetics. The liposomal delivery platform was further applied to enable the doxorubicin-mediated killing of a Langerin$^+$ monocyte cell line, highlighting its therapeutic and diagnostic potential in LCH. Beyond the envisioned applications in cancer immunotherapy and chemotherapy, the targeted liposomes also hold immediate value for investigations into the mechanisms of LC-mediated cross priming or tolerance induction as well as into the role of LCs in skin homeostasis.[50]

RESULTS

Heparin-Derived Monosaccharides Represent Favorable Scaffolds for Glycomimetic Ligand Design. Aside from its function as a pathogen recognition receptor, Langerin interacts with self-antigens such as glycosaminoglycans including heparin.[39,51−53] These linear polysaccharides are composed of disaccharide repeating units consisting of galactose or uronic acids and differentially sulfated *N*-acetyl glucosamine (GlcNAc). Prompted by the 10-fold affinity increase (K_D = 0.49 ± 0.05 mM) over mannose (Man) disaccharides (K_D = ca. 4 mM) recently reported for a heparin-derived trisaccharide, we employed ligand-observed ^{19}F R_2-filtered NMR experiments to determine K_I values for a set of differentially sulfated GlcNAc derivatives (Figure 1a).[38,39,54] Interestingly, the affinities of glucosamine-2-sulfate (GlcNS) (K_I = 1.4 ± 0.2 mM), *N*-acetyl glucosamine-6-sulfate (GlcNAc-6-OS) (K_I = 0.6 ± 0.1 mM), and glucosamine-2-sulfate-6-sulfate (GlcNS-6-OS) (K_I = 0.28 ± 0.06 mM) were comparable or higher than those observed for heparin-derived oligosaccharides and other monosaccharides including Glc (K_I = 21 ± 4 mM), GlcNAc (K_I = 4.1 ± 0.7 mM), and Man (K_I = 4.5 ± 0.5 mM) (Figure S1, Table S1).[52] Overall, our observations are in agreement with recently published results from surface plasmon resonance-based competition experiments.[55]

The affinity increase for GlcNS-6-OS, the most potent monosaccharide identified, is based on the formation of a salt bridge with K313 and a hydrogen bond with N307 by the sulfate group in C6, as previously shown by X-ray crystallography.[55] GlcNS-6-OS displayed an altered orientation of the Glc scaffold, characterized by an approximately 180° rotation, compared to the Langerin-GlcNAc complex, and no interactions were observed for the sulfate group in C2 (Figure 1b).[40] As this static model is contrasted by the additive structure−activity relationship (SAR) for the sulfation in C2 and C6, we propose the existence of alternative binding modes for sulfated GlcNAc derivatives, similar to the characteristics of Man recognition.[56] In addition, an H_2O-mediated hydrogen bond formed between the amide group in C2 and K299 is observed in the X-ray structure for GlcNAc and results in an affinity increase over Glc.[40]

Importantly, either of these interactions might be leveraged via the bioisosteric substitution of the sulfate groups in C2 or C6 with a sulfonamide linker, rendering sulfated GlcNAc derivatives favorable scaffolds for the design of glycomimetic Langerin ligands. In particular, the synthesis of GlcNS analogues represents an intriguing fragment growing approach to explore the carbohydrate binding site for favorable interactions (Figure 1a). We prioritized the introduction of substituents in C2 over C6 based on the synthetic feasibility. This design choices for our first-generation glycomimetics were further guided by the essential role of equatorial hydroxyl groups in C3 and C4 in Ca^+-dependent monosaccharide recognition and C1 being our preferred position for liposome conjugation.

Small Aromatic Sulfonamide Substituents Render Glycomimetics Potent Targeting Ligands for Langerin and Provide Specificity against DC-SIGN. Assuming the conservation of the Glc scaffold orientation observed for GlcNAc and based on the visual inspection of the carbohydrate binding site, small aromatic substituents in C2 were hypothesized to increase the affinity by the formation of cation-π interactions with K299 and K313 or $\pi-\pi$ and H-π interactions with F315 and P310, respectively (Figure 1b). Accordingly, a panel of GlcNS analogues **1**−**5** bearing differentially substituted phenyl rings was prepared, followed by the determination of K_I values (Figures 1a and S2, Scheme S1). The phenyl ring was chosen as an aromatic substituent

DOI: 10.1021/acscentsci.9b00093
ACS Cent. Sci. 2019, 5, 808−820

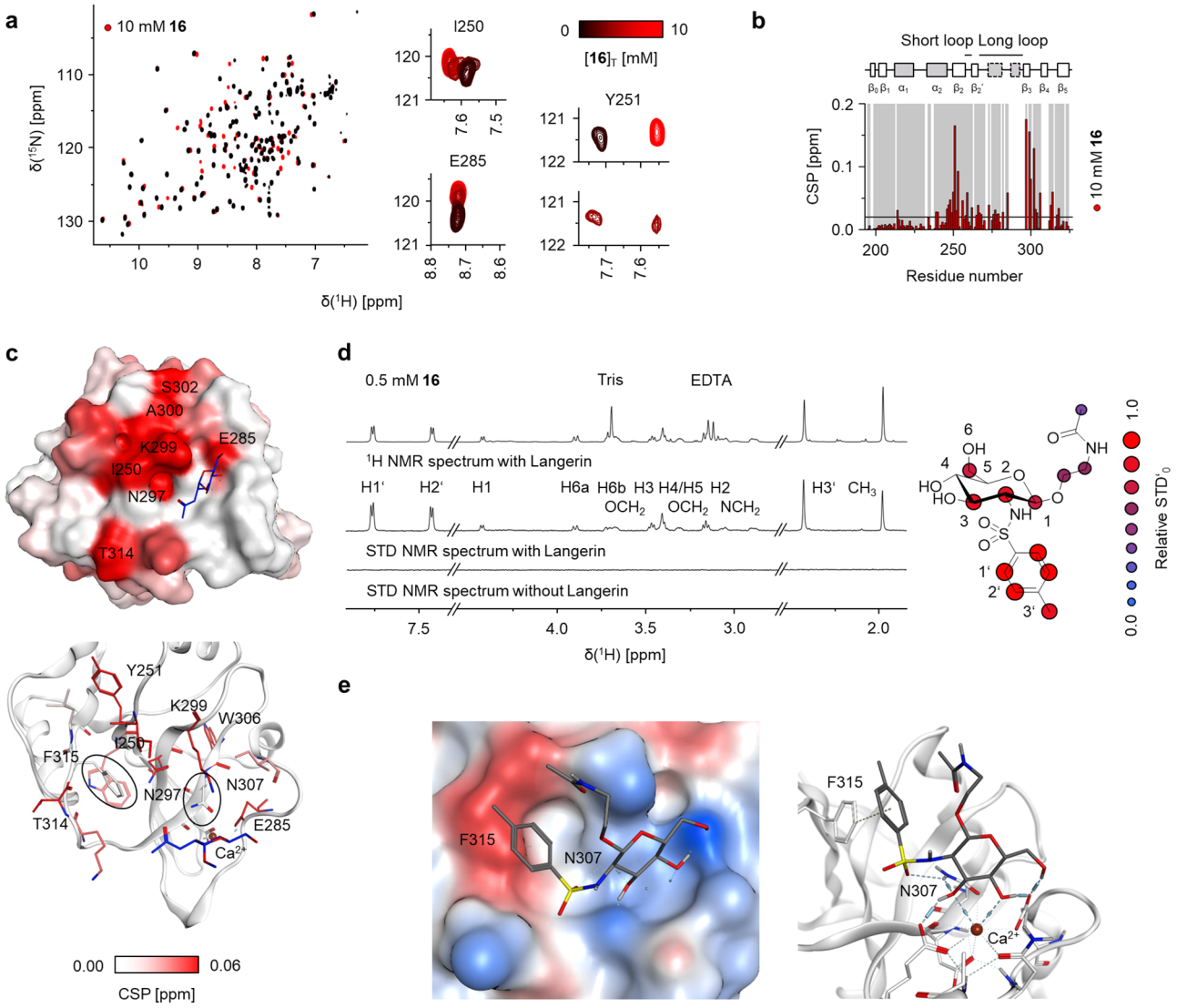

Figure 2. Binding mode analysis for the glycomimetic targeting ligand. (a and b) ^{15}N HSQC NMR experiments revealed the CSP pattern for **16**. Upon titration, fast-exchanging resonances such as I250 and E285 as well as slow-exchanging resonances including Y251 were observed. (c) Mapping the CSPs on the X-ray structure of Langerin in complex with GlcNAc (PDB code: 4N32) validated a Ca^{2+}-dependent binding mode as indicated by CSPs observed for E285 and K299.[40] Compared to titrations with **21**, Y251, I250, and T314 displayed a relative CSP increase, while a decrease was observed for K313 (Figure S6). Overall, the majority of residues displaying increased CSPs can be associated with N307 and F315, which could not be assigned[34] (d) STD NMR experiments served to further validate the interaction formed between **16** and Langerin. STD NMR spectra were recorded at saturation times t_{sat} of 0.4 s and are magnified 8-fold. Epitopes determined from build-up curves suggest strong interactions formed by the phenyl substituent (Figure S11). By contrast, low relative STD′$_0$ values were observed for the acetylated ethylamino linker, consistent with a solvent-exposed orientation. (e) **16** was docked into the carbohydrate binding site to rationalize the observations from ^{15}N HSQC and STD NMR experiments. The selected docking pose predicted the formation of $\pi-\pi$ interactions between the phenyl ring and F315 as well as the formation of a hydrogen bond between the sulfonamide group and N307. The linker displays high solvent exposure. The receptor surface is colored according to its lipophilicity (lipophilic: red, hydrophilic: blue).

with minimal steric demands, and methyl and chloride groups in para or meta were explored. Our selection aimed to test for steric tolerance in these positions while also evaluating the impact of electron-donating versus -withdrawing groups.

Increased affinities over GlcNAc were observed for all analogues, with a 13-fold affinity increase for **2** (K_I = 0.32 ± 0.05 mM), the most potent panel member (Figure S3, Table 1 and S2). The analogue bears a methyl group in para position of the phenyl ring that contributes minimally to the affinity increase, as exemplified by the K_I value obtained for **1** (K_I = 0.37 ± 0.04 mM). By comparison, **3** (K_I = 0.56 ± 0.09 mM), bearing the methyl group in meta, displays a decreased affinity, likely due to steric hindrance or the loss of rotational symmetry. The electron withdrawing chloride group in para of **4** (K_I = 0.60 ± 0.02 mM) also decreased the affinity, suggesting favorable contributions from H-π or $\pi-\pi$ interactions for **2**.[57]

Despite its low chemical complexity, **2** displays an affinity superior to that of glycans previously applied as targeting ligands for DC subsets distinct from LCs.[31] Here, the blood group antigen Le^X ($K_{D,DC\text{-}SIGN}$ = ca. 1 mM) was demonstrated to promote the DC-SIGN-dependent internalization of liposomes by isolated dermal DCs to activate T cells in vitro.[58] Encouraged by these reports, we advanced **2** toward targeted delivery applications via the introduction of an

DOI: 10.1021/acscentsci.9b00093
ACS Cent. Sci. 2019, 5, 808−820

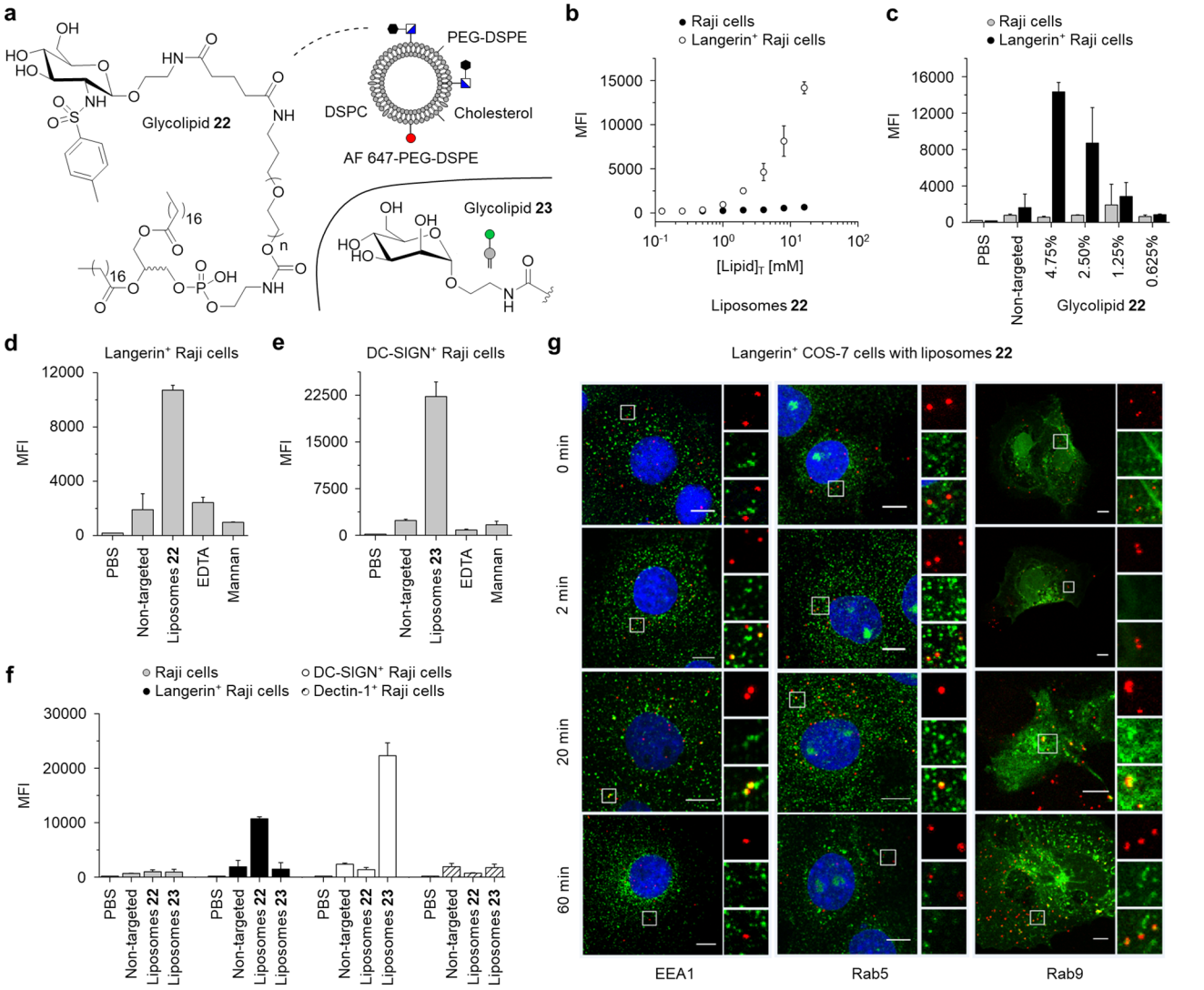

Figure 3. In vitro targeting of Langerin$^+$ human model cells. (a) Targeted liposomes were prepared by incorporating glycolipids **22** or **23** via thin film hydration and pore extrusion. The binding of the liposomes at 4 °C to human Raji cells expressing different CLRs was investigated by flow cytometry in three independent experiments. (b) Dose-dependent binding of liposomes **22** was observed for Langerin$^+$ cells using flow cytometry. The amount of liposomes used is expressed as the total concentration of lipids $[\text{Lipid}]_T$. All subsequent experiments were conducted at a concentration $[\text{Lipid}]_T$ of 16 μM. (c) Binding of liposomes **22** to Langerin$^+$ cells was furthermore dependent on the amount of the incorporated glycolipid. Only negligible unspecific binding of nontargeted liposomes to Raji cells was observed. All subsequent experiments were conducted at 4.75% of glycolipids **22** or **23**. (d) Competition experiments with EDTA and mannan validated Ca^{2+}-and carbohydrate binding site-dependent binding to Langerin$^+$ cells for liposomes **22**. (e) Analogously, liposomes **23**, bearing the Man on their surface, were observed to bind DC-SIGN$^+$ Raji cells via the Ca^{2+}-dependent carbohydrate binding site. (f) Among the set of analyzed CLRs including Langerin, DC-SIGN, and Dectin-1, liposomes **22** were found to be specific for Langerin$^+$ cells, while liposomes **23** exclusively bound to DC-SIGN$^+$ cells. (g) The intracellular trafficking of liposomes **22** (red) in Langerin$^+$ COS-7 cells was analyzed by confocal microscopy. Co-localization with the early endosomal compartment was observable 2 min after incubation at 37 °C using either the EEA-1 or the Rab5 marker (green). Liposomes remained associated with this compartment for at least 20 min. At this time point, a subset of liposomes was trafficked into the late endosomal compartment as indicated by the colocalization with the Rab9 marker (green). The scale bars indicate 10 μm.

ethylamino linker in β-orientation of C1 of the Glc scaffold to yield targeting ligand **15** (Figures 1a and S2, Scheme S2).

After acetylation of the amino group, we obtained model ligand **16** (Figure 1a and S2, Scheme S2). The K_I value determination for **16** (K_I = 0.24 ± 0.03 mM) revealed a 42-fold affinity increase over the Man-based reference molecule **21** (K_I = 10 ± 1 mM) (Figure 1a, 1c, S2 and S4, Table 1, Schemes S2 and S3). To validate these affinities and to expand our insight into the recognition process, orthogonal protein-observed ^{15}N HSQC NMR experiments were performed (Figures 1d, 2a and S5, Table 1). Notably, a considerable fraction of the resonances displaying chemical shift perturbations (CSPs) upon the addition of **16** also displayed line broadening $\Delta\nu_{0.5}$ of more than 10 Hz, indicative of intermediate exchange phenomena. Accordingly, these resonances were not considered for K_D determination. Simultaneously, slow exchange phenomena were observed for a set of resonances corresponding to Y251, I253, N297, and K299 (Figure 2a). Analysis of both fast- and slow-exchanging peaks revealed affinities comparable to the K_I values obtained for **16** ($K_{D,fast}$ = 0.23 ± 0.07 mM, $K_{D,slow}$ = 0.3 ± 0.1 mM) as well as **21** (K_D = 12 ± 1 mM) (Figures 1d and S5, Table 1). Likewise,

DOI: 10.1021/acscentsci.9b00093
ACS Cent. Sci. 2019, 5, 808−820

the affinity of **2** was validated using ^{15}N HSQC NMR ($K_{D,fast}$ = 0.46 ± 0.04 mM, $K_{D,slow}$ = 0.5 ± 0.2 mM) (Figure S6, Table 1).

Next, we explored the specificity of targeting ligand **16** against DC-SIGN as such off-target affinity would imply a reduced efficiency of the delivery approach and the potential induction of adverse effects. For this purpose, we transferred the ^{19}F R_2-filtered NMR reporter displacement assay to DC-SIGN (Figure S7, Table S3). Strikingly, **16** ($K_{I,DC\text{-}SIGN}$ = 15 ± 3 mM) displayed a considerably decreased K_I for DC-SIGN compared to Langerin corresponding to 63-fold specificity (Figure 1c, Table 1). At the same time, **21** displayed 3.7-fold specificity for DC-SIGN over Langerin ($K_{I,DC\text{-}SIGN}$ = 2.7 ± 0.3 mM). A comparison with the affinities determined for **2** ($K_{I,DC\text{-}SIGN}$ = 17 ± 1 mM) and Man ($K_{I,DC\text{-}SIGN}$ = 3.0 ± 0.3 mM) revealed that the differential recognition of α- and β-glycosides by these CLRs contributes to specificity (Figure S8, Table 1).

Formation of $\pi-\pi$ Interactions and Hydrogen Bonds by Aromatic Sulfonamide Substituents Mediates an Affinity Increase for Langerin. To investigate the binding mode of model ligand **16**, ^{15}N HSQC and STD NMR experiments were combined with molecular docking studies (Figure 2a−e). Here, the orientation of the linker was of particular interest to evaluate the compatibility of the binding mode with the presentation of targeting ligand **15** on liposomes.

Titration of **16** induced CSPs for E285 and K299 provided further evidence for a canonical Ca^{2+}-dependent binding mode of the Glc scaffold of the glycomimetic (Figure 2b,c). These protein-observed NMR experiments additionally revealed strong CSPs for residues in proximity of F315 and N307. Notably, both residues could not be assigned, likely due to their association with the flexible long loop.[34] This effect is accompanied by a decreased CSP for K313 compared to titrations with Man analogue **21** (Figures S5 and S9). Both observations are conserved in titrations with **2** and indicate an orientation of the phenyl ring toward F315 or K299 rather than K313 or P310 (Figures S6 and S9). Interestingly, additional CSPs were induced for residues remote from the carbohydrate binding, suggesting the modulation of an allosteric network involved in the regulation of Ca^{2+} recognition by Langerin (Note S1).[34]

To complement the protein-observed NMR experiments and to investigate the orientation of the acetylated ethylamino linker, STD NMR epitope mapping with **16** and **21** was conducted. The binding epitope of **16** was dominated by uniformly high STD effects for the phenyl ring and thus supports a model in which favorable secondary interactions are formed between this substituent and the Langerin surface (Figures 2d, S10 and S11). The acetylated ethylamino linker did, by contrast, display uniformly low STD effects indicating a solvent-exposed orientation and validating the developed conjugation strategy for GlcNS analogues. Similarly, the ethylamino linker of **21** received decreased STD effects compared to the Man scaffold (Figures S12 and S13).

Finally, molecular docking was performed utilizing the X-ray structure of the Langerin complex with GlcNAc (Figures 2e and S14).[40] Alternative conformations for K313 previously observed via X-ray crystallography were explicitly accounted for.[56] To address the challenging prediction of Ca^{2+}-dependent glycan−protein interactions, we employed a pharmacophore model constraining the orientation of the Glc scaffold during docking pose refinement and filtering.[46] Generated poses were evaluated in the context of the NMR experiments, and representative poses were selected to visualize the formation of potential secondary interactions. Indeed, orienting the phenyl ring toward F315 resulted in the formation of an edge-to-face $\pi-\pi$ interaction. This orientation also coincided with the formation of a weak hydrogen bond between the sulfonamide linker and N307. Both interactions explain the pronounced CSP values observed for residues that are associated with F315 and N307 including I250, Y251, N297, and K299. Furthermore, the phenyl ring received high STD effects indicating the formation of secondary interaction and high proximity to the Langerin surface. Conversely, the acetylated ethylamino linker displayed high solvent exposure and no conserved secondary interactions for the majority of docking poses. This observation was in accordance with the low STD effects and thus validated the developed conjugation strategy for GlcNS analogues. Overall, we propose a binding mode for **16** that displays a conserved orientation of the Glc scaffold, consistent with both STD and ^{15}N HSQC NMR experiments. The affinity increase can be rationalized by the formation of $\pi-\pi$ interactions between the phenyl substituent and F315 as well as a hydrogen bond between the sulfonamide linker and N297.

Targeted Liposomes Specifically Bind to Langerin$^+$ Cells in Vitro. Next, monosaccharide analogues **15** and **20** were utilized to synthesize glycolipids **22** and **23**, respectively (Figure 3a, Scheme S4). Their affinity for Langerin was evaluated in a plate-based enzyme-linked lectin assay (ELLA) (Figure S15).[31] While a dose-dependent interaction could be demonstrated for **22**, no interaction was detected for the immobilization of **23**. This validates the determined affinity increase of model ligand **16** over the Man-based reference molecule **21**. Encouraged by these findings, we prepared targeted liposomes labeled with Alexa Fluor (AF) 647 with a diameter d of 160 ± 60 nm that were stable over several months when stored at 4 °C in PBS (Figures 3a and S15). ^{1}H NMR experiments were employed to probe the accessibility of targeting ligand **15** on the surface of the liposomes. Interestingly, two states were observed for the resonances corresponding to H1′ and H2′ of the phenyl ring (Figure S15). Both states displayed line widths $\nu_{0.5}$ smaller than 30 Hz, suggesting residual flexibility due to the presentation of the targeting ligand on an extended polyethylene glycol linker. The alternative state potentially corresponds to targeting ligands oriented toward the lumen of the liposomes. In summary, **15** is likely presented favorably on the surface of the liposomes to enable interactions with Langerin, further validating the developed conjugation strategy.

The binding of the targeted liposomes to Langerin$^+$ Raji model cells was evaluated via flow cytometry (Figure S16). Indeed, initial titration experiments revealed dose- and Langerin-dependent binding of liposomes **22**, as well as negligible cytotoxicity (Figures 3b, S16 and S17). The avidity of the interaction was furthermore dependent on the fraction of glycolipid **22** incorporated into the liposomal formulation, with negligible unspecific interactions observed for non-targeted liposomes (Figure 3c). As expected, binding of the targeted liposomes could be abrogated via the addition of EDTA or the Man-based polysaccharide mannan to inhibit Ca^{2+}-dependent glycan recognition (Figure 3d). Analogously, liposomes **23**, bearing Man on their surface bound to DC-SIGN$^+$ Raji cells (Figure 3e). Strikingly, binding of these

DOI: 10.1021/acscentsci.9b00093
ACS Cent. Sci. 2019, 5, 808−820

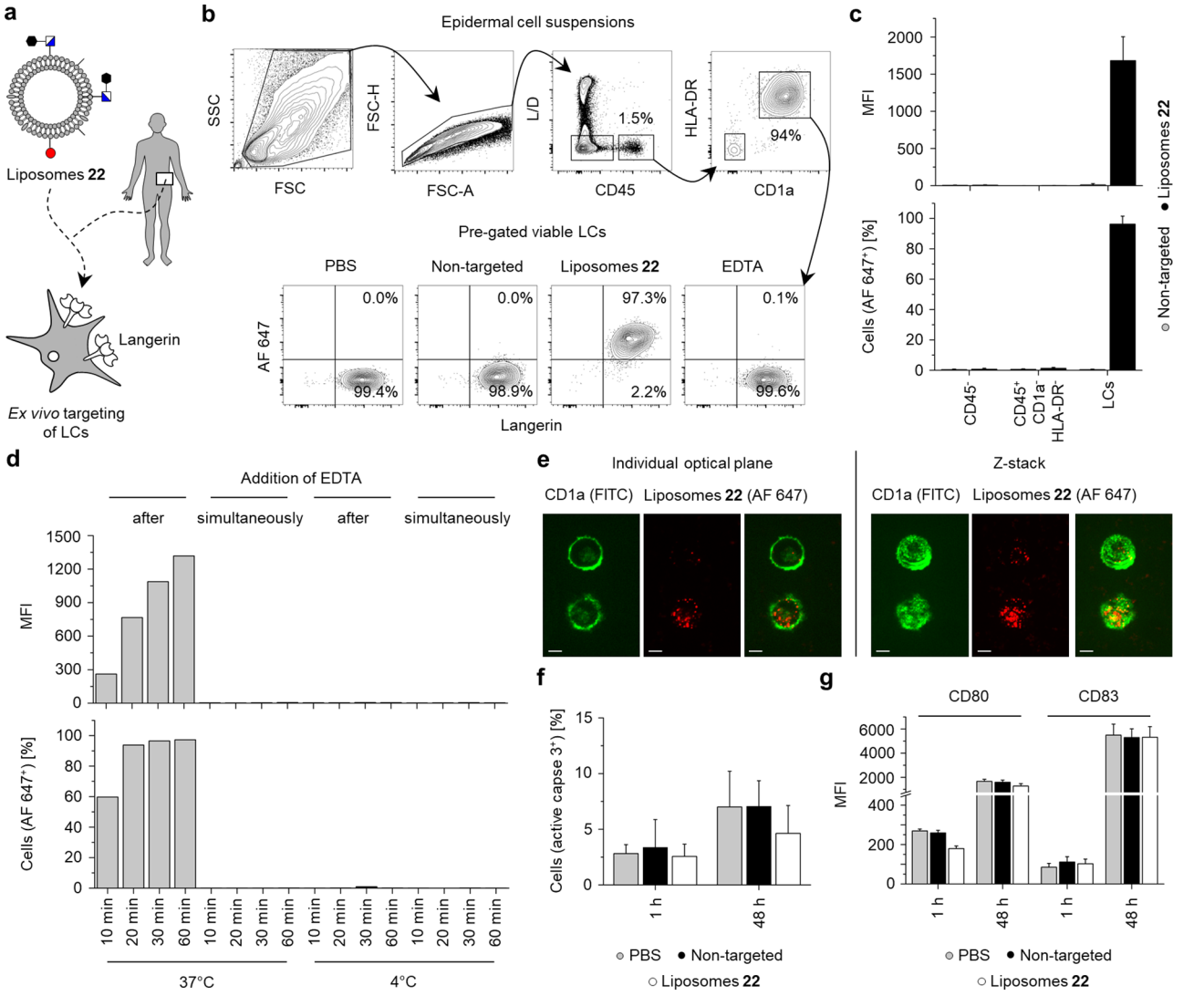

Figure 4. Ex vivo targeting of human LCs in epidermal cell suspensions. (a) LC targeting by liposomes **22** was investigated ex vivo using flow cytometry. To this end, epidermal cell suspensions were prepared as previously described and incubated at 37 °C.[60] (b and c) LCs were identified as viable HLA-DR$^+$-CD45$^+$-CD1a^{high} cells. The binding and endocytosis of liposomes **22** by human LCs was detected via the fluorescence signal of AF 647. Selectivity for LCs over CD45$^-$ keratinocytes and HLA-DR$^-$-CD45$^+$-CD1a$^-$ T cells was reproducibly demonstrated in four independent experiments and quantified via the fraction of AF 647$^+$ cells. The gating strategy is shown for one representative experiment. (d) The kinetics of endocytosis by LCs was analyzed at different temperatures in three independent experiments. Simultaneous incubation with liposomes **22** and EDTA resulted in complete inhibition of endocytosis. By contrast, the addition of EDTA 20 min after incubation at 37 °C did not alter the fraction of AF 647$^+$ LCs, indicating efficient endocytosis. As expected, endocytosis was abrogated at 4 °C. The results from one representative experiment are shown. (e) LCs in epidermal cell suspensions were identified by addition of a fluorescently labeled anti-CD1a antibody, and internalization of liposomes **22** was visualized by confocal microscopy at 37 °C. The scale bars indicate 4 μm. (f) The cytotoxicity of liposomes **22** for LCs was monitored in four independent experiments. No significant increase in active caspase 3 levels due to incubation with liposomes was observed after 1 or 48 h. (g) Furthermore, the incubation with liposomes **22** for 1 and 48 h in four independent experiments did not significantly increase the expression levels of CD80 or CD83, indicating the absence of liposome-mediated LC activation ex vivo.

liposomes was not detected for Langerin$^+$ or Dectin-1$^+$ cells, suggesting an avidity threshold for liposomal targeted delivery. These observations are consistent with the 3.7-fold specificity of Man-based reference molecule **21** for DC-SIGN over Langerin. Furthermore, DC-SIGN has been shown to form nanoclusters that specifically promote the binding and uptake of viruses and nanoparticles at the 100 nm scale.[59] Most importantly, Langerin-targeted liposomes specifically bound to Langerin$^+$ cells and neither to DC-SIGN nor Dectin-1 expressing cells (Figure 3f). The intracellular trafficking of liposomes **22** was followed in Langerin$^+$ COS-7 cells. Upon internalization, the liposomes colocalized with the early endosomal markers EEA1 and Rab5 within 2 min lasting up to at least 20 min (Figure 3g). At this later time point, a subset of liposomes was trafficked into the late endosomal compartment as demonstrated by costaining with Rab9 as a marker.

Langerhans Cells of the Human Epidermis Efficiently Internalize Targeted Liposomes. To explore the binding and subsequent internalization of the delivery platform by primary cells, we prepared epidermal cell suspensions from skin biopsies (Figure 4a).[60] The cells were incubated with targeted and nontargeted liposomes for 1 h at 37 °C and analyzed by flow cytometry. Upon incubation with liposomes **22**, more than 95% of gated HLA-DR$^+$-CD45$^+$-CD1a^{high} LCs

DOI: 10.1021/acscentsci.9b00093
ACS Cent. Sci. 2019, 5, 808−820

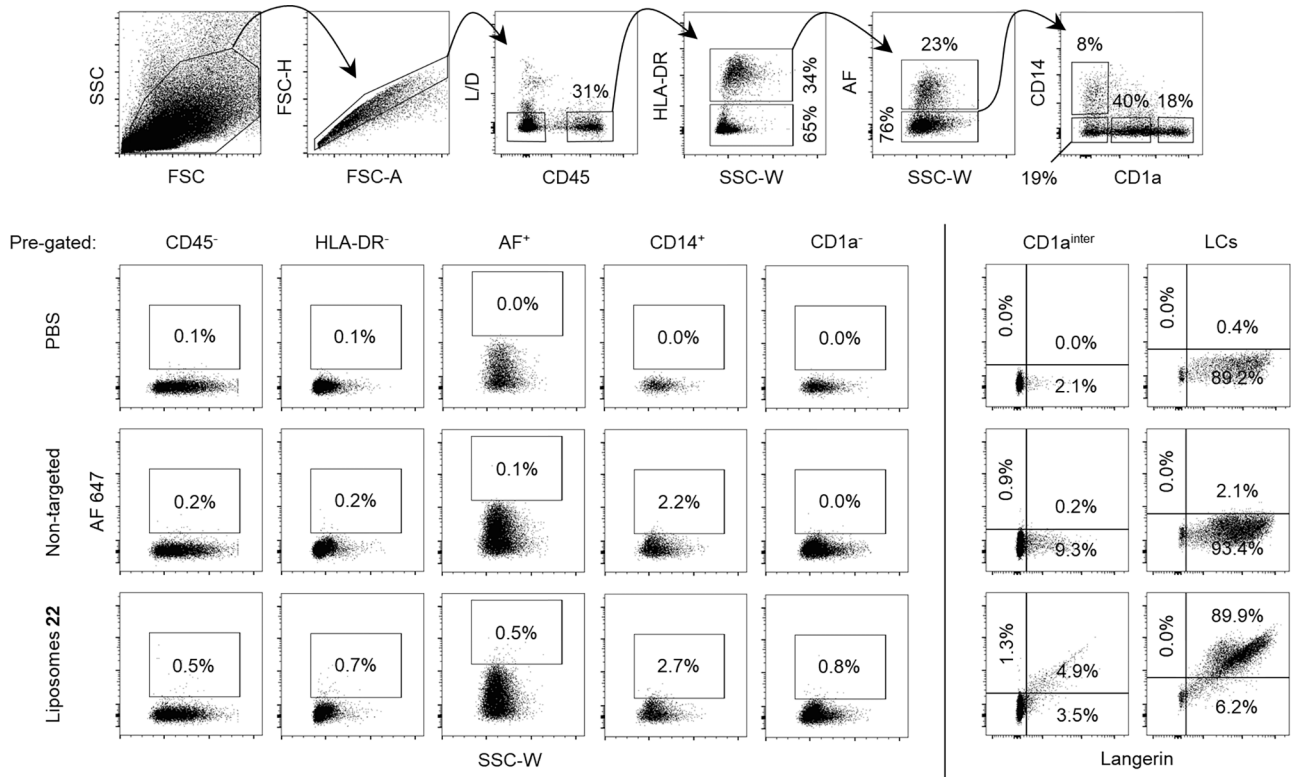

Figure 5. Ex vivo targeting of human LCs in whole skin cell suspensions. The specificity of liposomes **22** for LCs in the context of the human skin was evaluated at 37 °C by flow cytometry in three independent experiments. To this end, whole skin suspensions were prepared as previously published.[64] LCs were identified as viable HLA-DR$^+$-CD45$^+$-CD1a^{high} cells, while dermal DCs were identified as viable HLA-DR$^+$-CD45$^+$-CD1a^{intermediate} cells. Monocytes and macrophages were characterized by the expression of CD14. Strikingly, binding and endocytosis of liposomes **22** were exclusively observed for LCs. The results from one representative experiment are shown.

were found to display AF 647$^+$ fluorescence (Figure 4b). As for the Raji cells, binding was dependent on the targeting ligand and could be abrogated by simultaneous incubation with EDTA. The interaction was highly specific in the context of the human epidermis as neither keratinocytes nor T cells were targeted (Figure 4c).

Next, the kinetics of endocytosis by LCs were evaluated by adding EDTA at different times after the incubation with the delivery platform (Figure 4d). From these experiments, it can be inferred that more than 95% of gated LCs had internalized targeted liposomes after 20 min. The continuous increase in AF 647$^+$ fluorescence was monitored for up to 60 min, further highlighting the efficient endocytosis by LCs that was expectedly abrogated at 4 °C. The internalization of liposomes **22** was additionally demonstrated via confocal microscopy where only negligible colocalization with CD1a at the plasma membrane was observed (Figure 4e). Similar to the Langerin$^+$ Raji cells, the liposomal formulations displayed no cytotoxicity with LCs as indicated by the analysis of active caspase3 levels (Figures 4f and S18). Finally, we evaluated whether liposomes **22** would activate LCs ex vivo (Figures 4g and S18). The expression levels of neither CD80 nor CD83 were significantly increased after incubation with nontargeted or targeted liposomes for 1 h. As reported previously, LCs in epidermal cell suspension matured within 48 h, serving as an internal positive control.[61] This process was not affected by liposomes **22**. Additionally, we evaluated the induction of TNF-α secretion and did not observe liposome **22**-dependent LC activation after 16 h in this experiment (Figure S18). In conclusion, the targeted liposomes exclusively address Langerin$^+$ cells of the human skin while not inducing their activation.

As an alternative to epicutaneous administration, intradermal injection represents an attractive vaccination strategy for the skin.[25,62] However, the human dermis contains additional antigen-presenting cells including dermal DCs, macrophages, and monocytes. These cells express a variety of GBPs such as MR, Dectin-1, DC-SIGN, and Siglec-10 and hence represent potential targets for glycomimetics.[63] In analogy to the experiments with epidermal skin cell suspensions, whole skin cell suspensions were utilized to analyze the specificity of the delivery platform in a physiologically relevant context (Figure 5).[60] Again, targeted liposomes were efficiently endocytosed by LCs. Additionally, a minor population of CD1a^{intermediate}-Langerin$^+$ cells also capable of internalizing liposomes was identified. These cells might constitute a dermal DC subset but are most likely migrating LCs. Remarkably, endocytosis by CD1a^{intermediate}-Langerin$^-$ dermal DCs and other cell populations was negligible. Approximately 3% of CD14$^+$ macrophages and monocytes were targeted by liposomes **22**, comparable to the population nonspecifically internalizing nontargeted liposomes. Overall, the delivery platform was found to be highly specific for LCs in the context of the human skin.

Targeted Liposome-Mediated Delivery of Doxorubicin Exclusively Kills Langerin$^+$ Cells. To explore the modulation of cellular function using our liposomal delivery platform, we investigated the Langerin-specific killing of THP-1 cells in vitro in a colorimetric assay. As LCH is partially driven by the abnormal proliferation of Langerin$^+$ myeloid

DOI: 10.1021/acscentsci.9b00093
ACS Cent. Sci. 2019, 5, 808−820

progenitor cells, we have identified this dividing monocyte cell line as a viable experimental model for the disease. To this end, we encapsulated doxorubicin into liposomes as previously described (Figure 6a).[65] Incubation of Langerin$^+$ THP-1 cells

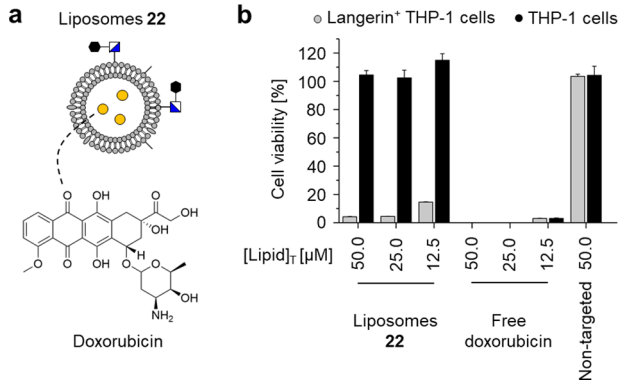

Figure 6. Specific doxorubicin-mediated killing of a Langerin$^+$ monocyte cell line in vitro. (a) The cytotoxic effect of liposome **22**-encapsulated doxorubicin on THP-1 cells, a monocyte cell line serving as a model for LCH, was investigated in a colorimetric assay in two independent experiments. (b) The cytotoxicity was specific for Langerin$^+$ cells and comparable to the incubation with free doxorubicin. In contrast, free doxorubicin killed both Langerin$^+$ and Langerin$^-$ cells, whereas incubation with nontargeted liposomes had no effect on either cell line. Free doxorubicin was used at concentrations corresponding to the total amount encapsulated in liposomes at a given $[Lipid]_T$. Liposomes **22** contained 0.225 equiv. of doxorubicin per $[Lipid]_T$. The results from one representative experiment are shown.

with liposomes **22** resulted in efficient killing at levels comparable to the use of free doxorubicin (Figure 6b). Importantly, no cytotoxicity was observed for Langerin$^-$ cells and the use of nontargeted liposomes in the tested concentration range. Our findings demonstrate the specific cell killing and the efficient intracellular release of cargo upon Langerin-dependent endocytosis.

DISCUSSION

Human LCs have been recognized for their capacity to internalize and cross-present exogenous antigens to elicit cytotoxic T cell responses, an established strategy for the development of novel cancer immunotherapies.[5,6] They reside in the epidermis of the skin and have consequently emerged as prime targets for transcutaneous vaccines.[7,25] However, the induction of protective T cell immunity remains challenging, requiring the efficient and specific delivery of antigens as well as adjuvants.[23,24] Moreover, lesions in LCH are predominantly composed of Langerin$^+$ myeloid progenitor cells, and current treatments of this pediatric cancer would benefit from the targeted delivery of chemotherapeutics to reduce adverse effects.[26] In this study, we present the development of a liposomal delivery platform that specifically addresses Langerin$^+$ cells, in particular in the context of the human skin, to overcome these challenges.

Beyond their relevance for transcutaneous vaccination strategies, our findings provide the proof of concept for CLR-mediated targeting of nanoparticles to individual immune cell subsets using glycomimetics. The discovery of ligand **15** (K_I = 0.24 ± 0.03 mM) with micromolar affinity for Langerin represents the essential innovation required to achieve efficient internalization of liposomes by LCs. Previous ex vivo studies have explored the use of natural glycans such as Le^Y for this purpose.[31] Interestingly, Le^Y did not promote endocytosis by LCs, while the Le^X-mediated ($K_{D,DC\text{-}SIGN}$ = ca. 1 mM) targeting of DC-SIGN on dermal DCs succeeded.[58] At the time, the authors concluded that liposomal formulations are not suitable to address LCs. Here, we propose the concept of CLR-specific avidity thresholds to explain these findings. The affinities of the utilized natural glycans for Langerin and DC-SIGN were comparable. Yet, the Le^X-bearing liposomespresumably displayed an increased avidity for dermal DCs due to the tetrameric organization of the carbohydrate recognition domains, the formation of nanoclusters, or increased expression levels for DC-SIGN.[59]

These characteristics render LCs more difficult targets for glycan-mediated liposomal delivery compared to dermal DCs. Here, we have demonstrated that this difficulty can be overcome by glycomimetic ligand design. While generally considered challenging in itself, the design of mono- or oligosaccharide analogues has been successfully applied to target delivery platforms to other GBPs such as ASGPR and Siglec-2.[66,67] The 42-fold affinity increase over natural glycans observed for **15**, by proxy of model ligand **16**, exceeds that reported for other first-generation glycomimetics and highlights the success of our heparin-inspired rational design strategy.[67−69] **15** additionally provides improved synthetic feasibility and metabolic stability over sulfated heparin-derived mono- (K_I = 0.28 ± 0.06 mM) or trisaccharides (K_D = 0.49 ± 0.05 mM), which display similar affinities.[39] Furthermore, we argue that the conjugation of GlcNS-6-OS to liposomes will result in an affinity decrease due to the loss of the hydrogen bond between the hydroxyl group in C1 and K299 recently observed via X-ray crystallography.[55] By comparison, the formation of β-glucosides represents a favorable conjugation strategy for the designed GlcNS analogues, superior to the use of α-mannosides previously explored.[54]

Using NMR spectroscopy and molecular docking, we have proposed a Ca^{2+}-dependent binding mode for **15**, which likely resembles that of GlcNAc.[40] The conserved orientation of the Glc scaffold allows for the formation of an edge-to-face $\pi-\pi$ interaction between the phenyl ring and F315 as well as a hydrogen bond between the sulfonamide linker and N307. The formation of the former interaction is further supported by the affinity decrease resulting from the introduction of the electron withdrawing chloride group for **4**.[57] The hydrogen bond with N307 was also observed for the sulfate group in C6 of GlcNS-O-6S via X-ray crystallography.[55] We conclude that these interactions contribute substantially to the affinity increase observed for **15**. The combination of the obtained SAR with our binding mode analysis will inform the design of next-generation glycomimetics. Attractive approaches to further optimize the affinity for Langerin include the introduction of electron-donating substituents in the para position on the phenyl ring such as amino or alkoxy groups will be evaluated to optimize the edge-to-face $\pi-\pi$ interaction between the phenyl ring and F315. Finally, the obtained SAR suggests that larger substituents extending in the para direction might be tolerated, and intriguing scaffolds for second-generation glycomimetics include biphenyl and naphthyl substituents. As our analysis does not account for conformational flexibility of the carbohydrate binding site and is furthermore limited by an incomplete resonance assignment for Langerin, X-ray

DOI: 10.1021/acscentsci.9b00093
ACS Cent. Sci. 2019, 5, 808−820

crystallography will serve to validate the proposed binding mode for **15** moving forward.

In summary, liposomes **22** bearing targeting ligand **15** were efficiently internalized both by model cells expressing Langerin as well as LCs in whole skin suspensions. Furthermore, we observed no cytotoxicity even upon exposure over several days. The kinetics of endocytosis were fast, and the majority of LCs was successfully addressed within 20 min, while internalization by off-target cells was negligible. Notably, the epidermis predominantly consists of keratinocytes, while LCs only amount to approximately 3% of epidermal cells.[70] Additional skin-resident immune cells such as dermal DCs and macrophages are present in the dermis, and many of these off-target cells express GBPs including CLRs such as MR, dectin-1, and DC-SIGN or Siglec-10.[63] Accordingly, the required specific delivery of antigens or adjuvants to LCs in the human skin is particularly challenging. Yet, **15** provided remarkable specificity for Langerin, despite its low chemical complexity. While residual off-target affinity can be expected for glycomimetic ligands, the proposed avidity threshold for liposomal targeting likely prevents endocytosis by non-LC skin-resident cells.[71] Intriguingly, our observation might be leveraged to infer general design principles for nanoparticle-based delivery platforms, emphasizing the monovalent specificity of targeting ligands. Overall, the reported findings not only highlight the therapeutic potential of the targeted liposomes, but also their value as molecular probes for basic research where they will potentially contribute to studying the role of LCs in skin homeostasis or to elucidate the mechanisms of antigen cross-presentation.[50]

In contrast to other CLRs, Langerin-dependent signaling has not been reported to date.[72] Our findings support this hypothesis as the binding and endocytosis of targeted liposomes did not activate immature LCs ex vivo. This expands the therapeutic scope of the liposomal delivery platform. On the one hand, the coadministration of adjuvants, preferably TLR-3 or MDA5 agonists, will promote the induction of cytotoxic T cell immunity required for cancer vaccines.[22,73,74] As both are intracellular pattern recognition receptors, facilitating the internalization of these agonists is of particular importance. On the other hand, antigen delivery to LCs in the absence of adjuvants has been shown to result in the expansion of regulatory T cells and can be leveraged to treat autoimmune diseases.[75] In this context, liposomes are superior to antibody−antigen conjugates as they enable the coformulation of antigens and adjuvants. While the systemic administration of adjuvants generally induces adverse effects and compromises cytotoxic T cell immunity, their targeted delivery to LCs allows for reduced adjuvant doses and tailored immune responses.

Moreover, many CLRs including Langerin recycle between the plasma membrane and the endosomal compartment.[35] In this context, the Ca^{2+}- and pH-dependent release of glycomimetic ligands in the early endosome increases the endocytic capacity of LCs and other DCs. It can be argued that this intracellular trafficking mechanism evolved to promote antigen cross-presentation.[76] The observed fast internalization kinetics and the prolonged colocalization of targeted liposomes with early endosomal markers suggest that this mechanism is efficiently exploited. By contrast, antibodies have been demonstrated to recycle back to the plasma membrane, thereby limiting the dose of internalized and processed antigens.[20,21] These characteristics highlight another potential advantage of the liposomal delivery platform over antibody-based approaches.

Future investigations will advance the Langerin-specific liposomal delivery platform toward in vivo studies. In this context, we explored the delivery of cargo to modulate cellular function in vitro. LCH, one of the most common pediatric cancers, is characterized by the formation of lesions of the skin, bone marrow, lungs, and other organs due to the abnormal proliferation of Langerin$^+$ myeloid progenitor cells.[26] As access to skin biopsies from pediatric cancer patients is highly restricted, we chose a monocyte cell line as an experimental model for the disease and were able to demonstrate Langerin-specific cytotoxicity of targeted liposomes containing doxorubicin. THP-1 cells are developmentally related to LCH cells and are, in contrast to LCs isolated from healthy individuals, highly proliferative, rendering them susceptible to cytostatic chemotherapeutics.[50] Our delivery platform also provides unique opportunities to improve current treatments of LCH. Specifically, these opportunities include the targeting of chemotherapeutics to lesions to improve the therapeutic window and the development of novel diagnostic tools to elucidate the mechanisms of disease progression.

Moving forward, we envision similar experiments ex vivo to demonstrate the LC-mediated induction of cytotoxic T cell responses. Important parameters of this process that remain to be investigated are the intracellular trafficking and the efficient cross-presentation of delivered antigen. Finally, the feasibility of transcutaneous vaccinations using targeted liposomes will be evaluated to pave the way for therapeutic applications.

Safety Statement. No unexpected or unusually high safety hazards were encountered.

■ ASSOCIATED CONTENT

Supporting Information

The Supporting Information is available free of charge on the ACS Publications website at DOI: 10.1021/acscentsci.9b00093.

Supporting notes, figures, tables, and schemes as well as methods (PDF)

■ AUTHOR INFORMATION

Corresponding Author

*E-mail: christoph.rademacher@mpikg.mpg.de.

ORCID

Oliver Seitz: 0000-0003-0611-4810

Christoph Rademacher: 0000-0001-7082-7239

Author Contributions

#J.S. and L.B. contributed equally.

Notes

The authors declare the following competing financial interest(s): E.-C.W., J.S., G.B., O.S. and C.R. declare the filing of a patent covering the use of glycomimetic Langerin ligands for targeting human Langerin-expressing cells.

■ ACKNOWLEDGMENTS

The work was financially supported for C.R. by the DFG (RA1944/2-1) and the Max Planck Society as well as by the Austrian Science Fund for P.S. (W1101-B15). We thank Prof. Dr. Peter H. Seeberger for support and helpful discussions. We would like to thank the Department of Plastic, Reconstructive and Aesthetic Surgery in Innsbruck for providing human skin

DOI: 10.1021/acscentsci.9b00093
ACS Cent. Sci. 2019, 5, 808−820

samples. N.M.S. was supported by the Dutch Scientific Organization (VIDI 91713303). Furthermore, we thank Dr. Dongyoon Kim for conducting preliminary microscopy experiments.

REFERENCES

(1) Prausnitz, M. R.; Langer, R. Transdermal drug delivery. *Nat. Biotechnol.* **2008**, *26* (11), 1261−1268.
(2) WHO expert committee on smallpox eradication. Second report. *World Health Organ Tech Rep. Ser.* 1972 *493* 1−64.
(3) Banchereau, J.; Steinman, R. M. Dendritic cells and the control of immunity. *Nature* **1998**, *392* (6673), 245−252.
(4) Clausen, B. E.; Stoitzner, P. Functional specialization of skin dendritic cell subsets in regulating T cell responses. *Front. Immunol.* **2015**, *6*, 534.
(5) Klechevsky, E.; Morita, R.; Liu, M.; Cao, Y.; Coquery, S.; Thompson-Snipes, L.; Briere, F.; Chaussabel, D.; Zurawski, G.; Palucka, A. K.; Reiter, Y.; Banchereau, J.; Ueno, H. Functional specializations of human epidermal Langerhans cells and CD14+ dermal dendritic cells. *Immunity* **2008**, *29* (3), 497−510.
(6) Stoitzner, P.; Tripp, C. H.; Eberhart, A.; Price, K. M.; Jung, J. Y.; Bursch, L.; Ronchese, F.; Romani, N. Langerhans cells cross-present antigen derived from skin. *Proc. Natl. Acad. Sci. U. S. A.* **2006**, *103* (20), 7783−7788.
(7) Zaric, M.; Lyubomska, O.; Poux, C.; Hanna, M. L.; McCrudden, M. T.; Malissen, B.; Ingram, R. J.; Power, U. F.; Scott, C. J.; Donnelly, R. F.; Kissenpfennig, A. Dissolving microneedle delivery of nanoparticle-encapsulated antigen elicits efficient cross-priming and Th1 immune responses by murine Langerhans cells. *J. Invest. Dermatol.* **2015**, *135* (2), 425−434.
(8) Kantoff, P. W.; Higano, C. S.; Shore, N. D.; Berger, E. R.; Small, E. J.; Penson, D. F.; Redfern, C. H.; Ferrari, A. C.; Dreicer, R.; Sims, R. B.; Xu, Y.; Frohlich, M. W.; Schellhammer, P. F.; for the IMPACT Study Investigators; et al. Sipuleucel-T immunotherapy for castration-resistant prostate cancer. *N. Engl. J. Med.* **2010**, *363* (5), 411−422.
(9) Thurner, B.; Haendle, I.; Roder, C.; Dieckmann, D.; Keikavoussi, P.; Jonuleit, H.; Bender, A.; Maczek, C.; Schreiner, D.; Von den Driesch, P.; Brocker, E. B.; Steinman, R. M.; Enk, A.; Kampgen, E.; Schuler, G. Vaccination with mage-3A1 peptide-pulsed mature, monocyte-derived dendritic cells expands specific cytotoxic T cells and induces regression of some metastases in advanced stage IV melanoma. *J. Exp. Med.* **1999**, *190* (11), 1669−1678.
(10) Garg, A. D.; Coulie, P. G.; Van den Eynde, B. J.; Agostinis, P. Integrating next-generation dendritic cell vaccines into the current cancer immunotherapy landscape. *Trends Immunol.* **2017**, *38* (8), 577−593.
(11) Bonifaz, L.; Bonnyay, D.; Mahnke, K.; Rivera, M.; Nussenzweig, M. C.; Steinman, R. M. Efficient targeting of protein antigen to the dendritic cell receptor DEC-205 in the steady state leads to antigen presentation on major histocompatibility complex class I products and peripheral CD8+ T cell tolerance. *J. Exp. Med.* **2002**, *196* (12), 1627−1638.
(12) Burgdorf, S.; Kautz, A.; Bohnert, V.; Knolle, P. A.; Kurts, C. Distinct pathways of antigen uptake and intracellular routing in CD4+ and CD8+ T cell activation. *Science* **2007**, *316* (5824), 612−616.
(13) Hartung, E.; Becker, M.; Bachem, A.; Reeg, N.; Jakel, A.; Hutloff, A.; Weber, H.; Weise, C.; Giesecke, C.; Henn, V.; Gurka, S.; Anastassiadis, K.; Mages, H. W.; Kroczek, R. A. Induction of potent CD8+ T cell cytotoxicity by specific targeting of antigen to cross-presenting dendritic cells in vivo via murine or human XCR1. *J. Immunol.* **2015**, *194* (3), 1069−1079.
(14) Steinman, R. M. Decisions about dendritic cells: past, present, and future. *Annu. Rev. Immunol.* **2012**, *30*, 1−22.
(15) Dhodapkar, M. V.; Sznol, M.; Zhao, B.; Wang, D.; Carvajal, R. D.; Keohan, M. L.; Chuang, E.; Sanborn, R. E.; Lutzky, J.; Powderly, J.; Kluger, H.; Tejwani, S.; Green, J.; Ramakrishna, V.; Crocker, A.; Vitale, L.; Yellin, M.; Davis, T.; Keler, T. Induction of antigen-specific immunity with a vaccine targeting NY-ESO-1 to the dendritic cell receptor DEC-205. *Sci. Transl. Med.* **2014**, *6* (232), 232ra51.
(16) Fehres, C. M.; Van Beelen, A. J.; Bruijns, S. C. M.; Ambrosini, M.; Kalay, H.; Bloois, L. V.; Unger, W. W. J.; Garcia-Vallejo, J. J.; Storm, G.; De Gruijl, T. D.; Kooyk, Y. V. In situ delivery of antigen to DC-SIGN+CD14+ dermal dendritic cells results in enhanced CD8+ T-cell responses. *J. Invest. Dermatol.* **2015**, *135* (9), 2228−2236.
(17) Tullett, K. M.; Leal Rojas, I. M.; Minoda, Y.; Tan, P. S.; Zhang, J. G.; Smith, C.; Khanna, R.; Shortman, K.; Caminschi, I.; Lahoud, M. H.; Radford, K. J. Targeting CLEC9A delivers antigen to human CD141+ DC for CD4+ and CD8+ T cell recognition. *JCI Insight* **2016**, *1* (7), 87102.
(18) Bonifaz, L. C.; Bonnyay, D. P.; Charalambous, A.; Darguste, D. I.; Fujii, S.; Soares, H.; Brimnes, M. K.; Moltedo, B.; Moran, T. M.; Steinman, R. M. In vivo targeting of antigens to maturing dendritic cells via the DEC-205 receptor improves T cell vaccination. *J. Exp. Med.* **2004**, *199* (6), 815−824.
(19) Herre, J.; Marshall, A. S.; Caron, E.; Edwards, A. D.; Williams, D. L.; Schweighoffer, E.; Tybulewicz, V.; Reise Sousa, C.; Gordon, S.; Brown, G. D. Dectin-1 uses novel mechanisms for yeast phagocytosis in macrophages. *Blood* **2004**, *104* (13), 4038−4045.
(20) Tacken, P. J.; Ginter, W.; Berod, L.; Cruz, L. J.; Joosten, B.; Sparwasser, T.; Figdor, C. G.; Cambi, A. Targeting DC-SIGN via its neck region leads to prolonged antigen residence in early endosomes, delayed lysosomal degradation, and cross-presentation. *Blood* **2011**, *118* (15), 4111−4119.
(21) O'Reilly, M. K.; Tian, H.; Paulson, J. C. CD22 is a recycling receptor that can shuttle cargo between the cell surface and endosomal compartments of B cells. *J. Immunol.* **2011**, *186* (3), 1554−1563.
(22) Fehres, C. M.; Duinkerken, S.; Bruijns, S. C.; Kalay, H.; Van Vliet, S. J.; Ambrosini, M.; De Gruijl, T. D.; Unger, W. W.; Garcia-Vallejo, J. J.; Van Kooyk, Y. Langerin-mediated internalization of a modified peptide routes antigens to early endosomes and enhances cross-presentation by human Langerhans cells. *Cell. Mol. Immunol.* **2017**, *14* (4), 360−370.
(23) Idoyaga, J.; Fiorese, C.; Zbytnuik, L.; Lubkin, A.; Miller, J.; Malissen, B.; Mucida, D.; Merad, M.; Steinman, R. M. Specialized role of migratory dendritic cells in peripheral tolerance induction. *J. Clin. Invest.* **2013**, *123* (2), 844−854.
(24) Flacher, V.; Tripp, C. H.; Mairhofer, D. G.; Steinman, R. M.; Stoitzner, P.; Idoyaga, J.; Romani, N. Murine Langerin+ dermal dendritic cells prime CD8+ T cells while Langerhans cells induce cross-tolerance. *EMBO Mol. Med.* **2014**, *6* (9), 1191−1204.
(25) Stoitzner, P.; Schaffenrath, S.; Tripp, C. H.; Reider, D.; Komenda, K.; Del Frari, B.; Djedovic, G.; Ebner, S.; Romani, N. Human skin dendritic cells can be targeted in situ by intradermal injection of antibodies against lectin receptors. *Exp Dermatol* **2014**, *23* (12), 909−915.
(26) Allen, C. E.; Merad, M.; McClain, K. L. Langerhans-cell histiocytosis. *N. Engl. J. Med.* **2018**, *379* (9), 856−868.
(27) Gadner, H.; Minkov, M.; Grois, N.; Potschger, U.; Thiem, E.; Arico, M.; Astigarraga, I.; Braier, J.; Donadieu, J.; Henter, J. I.; Janka-Schaub, G.; McClain, K. L.; Weitzman, S.; Windebank, K.; Ladisch, S. Therapy prolongation improves outcome in multisystem Langerhans cell histiocytosis. *Blood* **2013**, *121* (25), 5006−5014.
(28) Berres, M. L.; Lim, K. P.; Peters, T.; Price, J.; Takizawa, H.; Salmon, H.; Idoyaga, J.; Ruzo, A.; Lupo, P. J.; Hicks, M. J.; Shih, A.; Simko, S. J.; Abhyankar, H.; Chakraborty, R.; Leboeuf, M.; Beltrao, M.; Lira, S. A.; Heym, K. M.; Clausen, B. E.; Bigley, V.; Collin, M.; Manz, M. G.; McClain, K.; Merad, M.; Allen, C. E. BRAF-V600E expression in precursor versus differentiated dendritic cells defines clinically distinct LCH risk groups. *J. Exp. Med.* **2015**, *212* (2), 281.
(29) Barenholz, Y. Doxil(R) - the first FDA-approved nano-drug: lessons learned. *J. Controlled Release* **2012**, *160* (2), 117−134.
(30) Boks, M. A.; Ambrosini, M.; Bruijns, S. C.; Kalay, H.; Van Bloois, L.; Storm, G.; Garcia-Vallejo, J. J.; Van Kooyk, Y. MPLA incorporation into DC-targeting glycoliposomes favours anti-tumour T cell responses. *J. Controlled Release* **2015**, *216*, 37−46.

DOI: 10.1021/acscentsci.9b00093
ACS Cent. Sci. 2019, 5, 808−820

(31) Fehres, C. M.; Kalay, H.; Bruijns, S. C.; Musaafir, S. A.; Ambrosini, M.; Van Bloois, L.; Van Vliet, S. J.; Storm, G.; Garcia-Vallejo, J. J.; Van Kooyk, Y. Cross-presentation through Langerin and DC-SIGN targeting requires different formulations of glycan-modified antigens. *J. Controlled Release* **2015**, *203*, 67−76.
(32) Markov, O. V.; Mironova, N. L.; Shmendel, E. V.; Serikov, R. N.; Morozova, N. G.; Maslov, M. A.; Vlassov, V. V.; Zenkova, M. A. Multicomponent mannose-containing liposomes efficiently deliver RNA in murine immature dendritic cells and provide productive anti-tumour response in murine melanoma model. *J. Controlled Release* **2015**, *213*, 45−56.
(33) Macauley, M. S.; Pfrengle, F.; Rademacher, C.; Nycholat, C. M.; Gale, A. J.; Von Drygalski, A.; Paulson, J. C. Antigenic liposomes displaying CD22 ligands induce antigen-specific B cell apoptosis. *J. Clin. Invest.* **2013**, *123* (7), 3074−3083.
(34) Hanske, J.; Aleksic, S.; Ballaschk, M.; Jurk, M.; Shanina, E.; Beerbaum, M.; Schmieder, P.; Keller, B. G.; Rademacher, C. Intradomain allosteric network modulates calcium affinity of the C-type lectin receptor Langerin. *J. Am. Chem. Soc.* **2016**, *138* (37), 12176−12186.
(35) Mc Dermott, R.; Ziylan, U.; Spehner, D.; Bausinger, H.; Lipsker, D.; Mommaas, M.; Cazenave, J. P.; Raposo, G.; Goud, B.; De la Salle, H.; Salamero, J.; Hanau, D. Birbeck granules are subdomains of endosomal recycling compartment in human epidermal Langerhans cells, which form where Langerin accumulates. *Mol. Biol. Cell* **2002**, *13* (1), 317−335.
(36) Taylor, M. E.; Drickamer, K. Convergent and divergent mechanisms of sugar recognition across kingdoms. *Curr. Opin. Struct. Biol.* **2014**, *28*, 14−22.
(37) Stambach, N. S.; Taylor, M. E. Characterization of carbohydrate recognition by Langerin, a C-type lectin of Langerhans cells. *Glycobiology* **2003**, *13* (5), 401−410.
(38) Holla, A.; Skerra, A. Comparative analysis reveals selective recognition of glycans by the dendritic cell receptors DC-SIGN and Langerin. *Protein Eng., Des. Sel.* **2011**, *24* (9), 659−669.
(39) Munoz-Garcia, J. C.; Chabrol, E.; Vives, R. R.; Thomas, A.; De Paz, J. L.; Rojo, J.; Imberty, A.; Fieschi, F.; Nieto, P. M.; Angulo, J. Langerin-heparin interaction: two binding sites for small and large ligands as revealed by a combination of NMR spectroscopy and cross-linking mapping experiments. *J. Am. Chem. Soc.* **2015**, *137* (12), 4100−4110.
(40) Feinberg, H.; Rowntree, T. J.; Tan, S. L.; Drickamer, K.; Weis, W. I.; Taylor, M. E. Common polymorphisms in human Langerin change specificity for glycan ligands. *J. Biol. Chem.* **2013**, *288* (52), 36762−36771.
(41) Ernst, B.; Magnani, J. L. From carbohydrate leads to glycomimetic drugs. *Nat. Rev. Drug Discovery* **2009**, *8* (8), 661−677.
(42) Aretz, J.; Wamhoff, E. C.; Hanske, J.; Heymann, D.; Rademacher, C. Computational and experimental prediction of human C-type lectin receptor druggability. *Front. Immunol.* **2014**, *5*, 323.
(43) Hahm, H. S.; Schlegel, M. K.; Hurevich, M.; Eller, S.; Schuhmacher, F.; Hofmann, J.; Pagel, K.; Seeberger, P. H. Automated glycan assembly using the Glyconeer 2.1 synthesizer. *Proc. Natl. Acad. Sci. U. S. A.* **2017**, *114* (17), E3385−E3389.
(44) Lenci, E.; Menchi, G.; Trabocchi, A. Carbohydrates in diversity-oriented synthesis: challenges and opportunities. *Org. Biomol. Chem.* **2016**, *14* (3), 808−825.
(45) Mangold, S. L.; Prost, L. R.; Kiessling, L. L. Quinoxalinone Inhibitors of the Lectin DC-SIGN. *Chem. Sci.* **2012**, *3* (3), 772−777.
(46) Nycholat, C. M.; Rademacher, C.; Kawasaki, N.; Paulson, J. C. In silico-aided design of a glycan ligand of sialoadhesin for in vivo targeting of macrophages. *J. Am. Chem. Soc.* **2012**, *134* (38), 15696−15699.
(47) Egger, J.; Weckerle, C.; Cutting, B.; Schwardt, O.; Rabbani, S.; Lemme, K.; Ernst, B. Nanomolar E-selectin antagonists with prolonged half-lives by a fragment-based approach. *J. Am. Chem. Soc.* **2013**, *135* (26), 9820−9828.
(48) Aretz, J.; Anumala, U. R.; Fuchsberger, F. F.; Molavi, N.; Ziebart, N.; Zhang, H.; Nazare, M.; Rademacher, C. Allosteric inhibition of a mammalian lectin. *J. Am. Chem. Soc.* **2018**, *140* (44), 14915−14925.
(49) Sommer, R.; Wagner, S.; Rox, K.; Varrot, A.; Hauck, D.; Wamhoff, E. C.; Schreiber, J.; Ryckmans, T.; Brunner, T.; Rademacher, C.; Hartmann, R. W.; Bronstrup, M.; Imberty, A.; Titz, A. Glycomimetic, orally bioavailable LecB inhibitors block biofilm formation of Pseudomonas aeruginosa. *J. Am. Chem. Soc.* **2018**, *140* (7), 2537−2545.
(50) Romani, N.; Clausen, B. E.; Stoitzner, P. Langerhans cells and more: Langerin-expressing dendritic cell subsets in the skin. *Immunol. Rev.* **2010**, *234* (1), 120−141.
(51) Zhao, J.; Liu, X.; Kao, C.; Zhang, E.; Li, Q.; Zhang, F.; Linhardt, R. J. Kinetic and structural studies of interactions between glycosaminoglycans and Langerin. *Biochemistry* **2016**, *55* (32), 4552−4559.
(52) Hanske, J.; Wawrzinek, R.; Geissner, A.; Wamhoff, E. C.; Sellrie, K.; Schmidt, H.; Seeberger, P. H.; Rademacher, C. Calcium-independent activation of an allosteric network in Langerin by heparin oligosaccharides. *ChemBioChem* **2017**, *18* (13), 1183−1187.
(53) Chabrol, E.; Nurisso, A.; Daina, A.; Vassal-Stermann, E.; Thepaut, M.; Girard, E.; Vives, R. R.; Fieschi, F. Glycosaminoglycans are interactants of Langerin: comparison with gp120 highlights an unexpected calcium-independent binding mode. *PLoS One* **2012**, *7* (11), e50722.
(54) Wamhoff, E. C.; Hanske, J.; Schnirch, L.; Aretz, J.; Grube, M.; Varon Silva, D.; Rademacher, C. 19F NMR-Guided Design of Glycomimetic Langerin Ligands. *ACS Chem. Biol.* **2016**, *11* (9), 2407−2413.
(55) Porkolab, V.; Chabrol, E.; Varga, N.; Ordanini, S.; Sutkeviciu Te, I.; Thepaut, M.; Garcia-Jimenez, M. J.; Girard, E.; Nieto, P. M.; Bernardi, A.; Fieschi, F. Rational-differential design of highly specific glycomimetic ligands: targeting DC-SIGN and excluding Langerin recognition. *ACS Chem. Biol.* **2018**, *13* (3), 600−608.
(56) Feinberg, H.; Taylor, M. E.; Razi, N.; McBride, R.; Knirel, Y. A.; Graham, S. A.; Drickamer, K.; Weis, W. I. Structural basis for langerin recognition of diverse pathogen and mammalian glycans through a single binding site. *J. Mol. Biol.* **2011**, *405* (4), 1027−1039.
(57) Martinez, C. R.; Iverson, B. L. Rethinking the term "pi-stacking. *Chem. Sci.* **2012**, *3* (7), 2191−2201.
(58) Pederson, K.; Mitchell, D. A.; Prestegard, J. H. Structural characterization of the DC-SIGN−LeX complex. *Biochemistry* **2014**, *53* (35), 5700−5709.
(59) Manzo, C.; Torreno-Pina, J. A.; Joosten, B.; Reinieren-Beeren, I.; Gualda, E. J.; Loza-Alvarez, P.; Figdor, C. G.; Garcia-Parajo, M. F.; Cambi, A. The neck region of the C-type lectin DC-SIGN regulates its surface spatiotemporal organization and virus-binding capacity on antigen-presenting cells. *J. Biol. Chem.* **2012**, *287* (46), 38946−38955.
(60) Stoitzner, P.; Romani, N.; McLellan, A. D.; Tripp, C. H.; Ebner, S. Isolation of skin dendritic cells from mouse and man. *Methods Mol. Biol.* **2010**, *595*, 235−248.
(61) Ebner, S.; Nguyen, V. A.; Forstner, M.; Wang, Y. H.; Wolfram, D.; Liu, Y. J.; Romani, N. Thymic stromal lymphopoietin converts human epidermal Langerhans cells into antigen-presenting cells that induce proallergic T cells. *J. Allergy Clin. Immunol.* **2007**, *119* (4), 982−990.
(62) Romani, N.; Thurnher, M.; Idoyaga, J.; Steinman, R. M.; Flacher, V. Targeting of antigens to skin dendritic cells: possibilities to enhance vaccine efficacy. *Immunol. Cell Biol.* **2010**, *88* (4), 424−430.
(63) Teunissen, M. B.; Haniffa, M.; Collin, M. P. Insight into the immunobiology of human skin and functional specialization of skin dendritic cell subsets to innovate intradermal vaccination design. *Curr. Top. Microbiol. Immunol.* **2011**, *351*, 25−76.
(64) Gunawan, M.; Jardine, L.; Haniffa, M. Isolation of human skin dendritic cell subsets. In *Dendritic Cell Protocols*; Segura, E., Onai, N., Eds.; Springer New York: New York, NY, 2016; pp 119−128.

DOI: 10.1021/acscentsci.9b00093
ACS Cent. Sci. 2019, 5, 808−820

(65) Chen, W. C.; Completo, G. C.; Sigal, D. S.; Crocker, P. R.; Saven, A.; Paulson, J. C. In vivo targeting of B-cell lymphoma with glycan ligands of CD22. *Blood* **2010**, *115* (23), 4778−4786.
(66) Peng, W.; Paulson, J. C. CD22 ligands on a natural N-glycan scaffold efficiently deliver toxins to B-lymphoma cells. *J. Am. Chem. Soc.* **2017**, *139* (36), 12450−12458.
(67) Sanhueza, C. A.; Baksh, M. M.; Thuma, B.; Roy, M. D.; Dutta, S.; Preville, C.; Chrunyk, B. A.; Beaumont, K.; Dullea, R.; Ammirati, M.; Liu, S.; Gebhard, D.; Finley, J. E.; Salatto, C. T.; King-Ahmad, A.; Stock, I.; Atkinson, K.; Reidich, B.; Lin, W.; Kumar, R.; Tu, M.; Menhaji-Klotz, E.; Price, D. A.; Liras, S.; Finn, M. G.; Mascitti, V. Efficient liver targeting by polyvalent display of a compact ligand for the Asialoglycoprotein Receptor. *J. Am. Chem. Soc.* **2017**, *139* (9), 3528−3536.
(68) Thepaut, M.; Guzzi, C.; Sutkeviciute, I.; Sattin, S.; Ribeiro-Viana, R.; Varga, N.; Chabrol, E.; Rojo, J.; Bernardi, A.; Angulo, J.; Nieto, P. M.; Fieschi, F. Structure of a glycomimetic ligand in the carbohydrate recognition domain of C-type lectin DC-SIGN. Structural requirements for selectivity and ligand design. *J. Am. Chem. Soc.* **2013**, *135* (7), 2518−2529.
(69) Hauck, D.; Joachim, I.; Frommeyer, B.; Varrot, A.; Philipp, B.; Möller, H. M.; Imberty, A.; Exner, T. E.; Titz, A. Discovery of two classes of potent glycomimetic inhibitors of Pseudomonas aeruginosa LecB with distinct binding modes. *ACS Chem. Biol.* **2013**, *8* (8), 1775−1784.
(70) Bauer, J.; Bahmer, F. A.; Worl, J.; Neuhuber, W.; Schuler, G.; Fartasch, M. A strikingly constant ratio exists between Langerhans cells and other epidermal cells in human skin. A stereologic study using the optical disector method and the confocal laser scanning microscope. *J. Invest. Dermatol.* **2001**, *116* (2), 313−318.
(71) Scharenberg, M.; Schwardt, O.; Rabbani, S.; Ernst, B. Target selectivity of FimH antagonists. *J. Med. Chem.* **2012**, *55* (22), 9810−9816.
(72) Geijtenbeek, T. B.; Gringhuis, S. I. Signalling through C-type lectin receptors: shaping immune responses. *Nat. Rev. Immunol.* **2009**, *9* (7), 465−479.
(73) Oosterhoff, D.; Heusinkveld, M.; Lougheed, S. M.; Kosten, I.; Lindstedt, M.; Bruijns, S. C.; Van Es, T.; Van Kooyk, Y.; Van der Burg, S. H.; De Gruijl, T. D. Intradermal delivery of TLR agonists in a human explant skin model: preferential activation of migratory dendritic cells by polyribosinic-polyribocytidylic acid and peptidoglycans. *J. Immunol.* **2013**, *190* (7), 3338−3345.
(74) Flacher, V.; Bouschbacher, M.; Verronese, E.; Massacrier, C.; Sisirak, V.; Berthier-Vergnes, O.; De Saint-Vis, B.; Caux, C.; Dezutter-Dambuyant, C.; Lebecque, S.; Valladeau, J. Human Langerhans cells express a specific TLR profile and differentially respond to viruses and Gram-positive bacteria. *J. Immunol.* **2006**, *177* (11), 7959−7967.
(75) Seneschal, J.; Clark, R. A.; Gehad, A.; Baecher-Allan, C. M.; Kupper, T. S. Human epidermal Langerhans cells maintain immune homeostasis in skin by activating skin resident regulatory T cells. *Immunity* **2012**, *36* (5), 873−884.
(76) Fehres, C. M.; Unger, W. W.; Garcia-Vallejo, J. J.; Van Kooyk, Y. Understanding the biology of antigen cross-presentation for the design of vaccines against cancer. *Front. Immunol.* **2014**, *5*, 149.

DOI: 10.1021/acscentsci.9b00093
ACS Cent. Sci. 2019, 5, 808−820